

Gravitational chargegenesis

Martin A. Mojahed ^{1,2,*} Kai Schmitz ^{3,†} and Xun-Jie Xu ^{4,‡}¹*Physik-Department T70, Technische Universität München,
James-Frank-Straße 1, D-85748 Garching, Germany*²*PRISMA⁺ Cluster of Excellence and Mainz Institute for Theoretical Physics
Johannes Gutenberg University, 55099 Mainz, Germany*³*Institute for Theoretical Physics, University of Münster, 48149 Münster, Germany*⁴*Institute of High Energy Physics, Chinese Academy of Sciences, Beijing 100049, China*

(Dated: September 18, 2024)

Wash-in leptogenesis is an attractive mechanism to produce the baryon asymmetry of the Universe. It treats right-handed-neutrino interactions as spectator processes, on the same footing as electroweak sphalerons, that reprocess primordial charge asymmetries in the thermal plasma into a baryon-minus-lepton asymmetry. The origin of these primordial charges must be accounted for by new CP -violating dynamics at very high energies. In this paper, we propose such a scenario of chargegenesis that, unlike earlier proposals, primarily relies on new interactions in the gravitational sector. We point out that a coupling of a conserved current to the divergence of the Ricci scalar during reheating can lead to nonzero effective chemical potentials in the plasma that, together with a suitable charge-violating interaction, can result in the production of a primordial charge asymmetry. Gravitational chargegenesis represents a substantial generalization of the idea of gravitational baryogenesis. We provide a detailed analysis of a generic and minimal realization that is consistent with inflation and show that it can successfully explain the baryon asymmetry of the Universe.

I. INTRODUCTION

The excess of matter over antimatter in our Universe [1] provides evidence for new physics beyond the Standard Model (SM), and its origin remains an open question. A popular class of mechanisms for dynamically generating the baryon asymmetry in the early universe (BAU) is known as leptogenesis [2], which requires an extension of the SM field content by right-handed neutrinos (RHNs). Most realizations of the leptogenesis idea rely on both charge-parity (CP) violation and out-of-equilibrium $B-L$ -violating interactions — two essential ingredients for the generation of the BAU — to emerge from the RHN sector [3]. The recent wash-in leptogenesis proposal [4, 5], however, is an exception to this lore, which allows a hierarchy between the temperature scales of CP and $B-L$ violation and does not require any CP violation from the RHN sector.

At the core of wash-in leptogenesis lies the idea of considering non-trivial chemical background configurations in the early Universe and treating RHNs on par with electroweak (EW) sphalerons. Analogous to how sphalerons act on the chemical background to wash in a $B+L$ asymmetry, the RHNs act as spectator fields providing a new equilibrium attractor for the chemical potentials that generically features nonzero $B-L$, even if $B-L=0$ initially [4]. As the wash-in leptogenesis mechanism requires a non-trivial chemical background as an initial condition to wash in a $B-L$ asymmetry, it only qualifies as a full theory of baryogenesis when accom-

panied by ultraviolet (UV) dynamics that can generate the chemical background. The UV completion of wash-in leptogenesis may be referred to as *chargegenesis*: a mechanism that provides the necessary CP -violating initial conditions for wash-in leptogenesis, but which itself may still conserve the $B-L$ charge of the Universe.

Thus far, several scenarios of chargegenesis have been studied in the literature, including axion inflation [5], heavy Higgs decays [6], and the evaporation of primordial black holes [7]. Common to all of these studies is that they rely on particle dynamics. In the present work, we shall propose a new avenue for chargegenesis — *gravitational chargegenesis* — in which gravity takes center stage.

Our gravitational chargegenesis setup shares similarities with gravitational baryogenesis, which is based on an effective interaction of the following form [8]

$$\mathcal{L} \supset \frac{1}{M_*^2} \int d^4x \sqrt{-g} J_A^\mu \partial_\mu \mathcal{R}, \quad (1)$$

where \mathcal{R} is the Ricci scalar, M_* parametrizes the UV scale relevant to the generation of this interaction, and J_A denotes a generic current, which in gravitational baryogenesis is the baryon current. In our mechanism, by contrast, A can be any of the SM global charges that are conserved in the SM plasma at high temperatures and that can be employed in wash-in leptogenesis.

In the FLRW Universe, Eq. (1) leads to an effective chemical potential associated with the current J_A ,

$$\mu_A^{\text{eff}} = \frac{\dot{\mathcal{R}}}{M_*^2} = \frac{3\rho\dot{\omega}}{M_*^2 M_P^2} + \frac{\sqrt{3}(1+\omega)(1-3\omega)}{M_*^2 M_P^3} \rho^{\frac{3}{2}}, \quad (2)$$

where $\dot{\mathcal{R}}$ is the time derivative of the Ricci scalar, M_P is the reduced Planck mass, ρ denotes the energy density

* mojahedm@uni-mainz.de

† kai.schmitz@uni-muenster.de

‡ xuj@ihep.ac.cn

of the Universe, and ω is the equation-of-state (EOS) parameter, i.e. the ratio of pressure and energy density. The effective chemical potential μ_A^{eff} induces non-vanishing chemical potentials μ_i for all particle species i carrying an A charge. In general, these particle species also carry other global charges. If one of these charges, say C , should be violated by an interaction in the plasma, the bias introduced by the chemical potentials $\mu_i \propto \mu_A^{\text{eff}}$ will hence lead to the generation of a nonzero charge asymmetry in equilibrium, q_C^{eq} . The exact relation between q_C^{eq} and μ_A^{eff} depends on the susceptibility matrix of the plasma, χ_{CA} , see Eq. (2.31) in Ref. [9] for an explicit expression that can be readily applied to our scenario.

While the origin of the interaction in Eq. (1) was originally envisioned to arise from quantum gravity, it was later argued that an effective interaction of this form is a generic outcome in models that feature high-scale CP violation in a curved spacetime background, which can result in a cutoff scale $M_* \ll M_P$ [10–13]. In fact, a theory of gravitational leptogenesis was studied previously, where A was identified with lepton number [10–16]. It was shown that the interaction (1) is generated dynamically at two loops in the type-I seesaw mechanism [17–20] when the seesaw Lagrangian is minimally coupled to the gravitational background as a direct consequence of CP violation in the RHN Yukawa sector. When combined with lepton-number violation in the RHN sector, this provided a new contribution to leptogenesis. Here, we point out that the charge A associated with the current in Eq. (1) and the charge C that is being violated do *not* have to be the same charge, which relaxes the assumptions required for successful baryogenesis via chargegenesis. Additionally, the RHN sector is liberated from CP violation constraints, as the RHNs are only required to wash in a nonzero $B - L$ asymmetry.

The effective chemical potential in Eq. (2) vanishes if $\omega = -1$ or $\omega = 1/3$, which implies that when the Universe is dominated by vacuum energy (e.g., during inflation) or radiation, the gravitationally generated chemical potential is suppressed. The suppression can be alleviated by enhancing the trace anomaly of the energy-momentum tensor, e.g., by adding many new particles charged under a new $SU(N)$ gauge group to the thermal plasma [8]. Alternatively, one may replace \mathcal{R} in Eq. (1) by a scalar function $f(\mathcal{R})$ [21, 22], or modified theories of gravity [23–28], see also Refs. [29, 30] for related ideas.

In the present work, we consider a simple framework to evade the large suppression of \mathcal{R} that relies on nothing but the oscillations of the inflaton field ϕ during the stage of reheating after inflation. After a period of slow-roll inflation driven by ϕ rolling down its potential $V(\phi)$, ϕ starts oscillating around the minimum of its potential. If the potential can be approximated as a monomial around its minimum, $V(\phi) \approx \phi^p$, the EOS parameter reads $\omega \approx (p - 2)/(p + 2)$ [31], which in general differs from $1/3$ or -1 . As we will show, this renders the gravitational chargegenesis mechanism compatible with high-scale inflationary setups, without modifying gravity or

adding extra particle species to the thermal plasma. We also provide a detailed time-resolved picture of how the charge asymmetry is generated as the Universe transitions from a period of inflation to reheating and beyond. Throughout this work, we employ Planck units, $M_P = 1$.

II. EQUATIONS AND SOLUTIONS

The evolution of the inflaton field ϕ , the radiation energy density ρ_R , and the charge asymmetry q_C is described by the following set of equations,

$$\ddot{\phi} + (3H + \Gamma_\phi)\dot{\phi} = -\frac{dV}{d\phi}, \quad (3)$$

$$\dot{\rho}_R + 4H\rho_R = \Gamma_\phi(\rho_\phi + p_\phi), \quad (4)$$

$$\dot{q}_C + 3Hq_C = \Gamma_C(q_C^{\text{eq}} - q_C). \quad (5)$$

Here, H is the Hubble parameter, V is the inflaton potential, Γ_ϕ is the decay rate of ϕ to radiation, $\rho_\phi = \frac{1}{2}\dot{\phi}^2 + V$ and $p_\phi = \frac{1}{2}\dot{\phi}^2 - V$ are the inflaton energy density and pressure, and Γ_C is the rate of the charge-violating process that drives q_C towards its equilibrium value q_C^{eq} . In general, we have $q_C^{\text{eq}} = \chi_{CA}T^2\mu_A^{\text{eff}}/6$, with the susceptibilities χ_{CA} depending on the exact choice of A and C and the temperature scale of chargegenesis. The nonzero entries of χ_{CA} are, however, typically of $\mathcal{O}(1)$. For definiteness, we will therefore simply work with $q_C^{\text{eq}} = T^2\mu_A^{\text{eff}}/6$ in the following.

We parametrize the reaction rate Γ_C in a model-independent way in terms of an energy scale M_C ,

$$\Gamma_C = \frac{T^{2n+1}}{M_C^{2n}}, \quad (6)$$

where n is a positive integer. Eq. (6) may stem from an effective operator \mathcal{O}_C with mass dimension $D = 4 + n$. For convenience, we also define the charge density in a comoving volume, $Q_C \equiv q_C(a/a_i)^3$ and $Q_C^{\text{eq}} \equiv q_C^{\text{eq}}(a/a_i)^3$ with a the FLRW scale factor, and a_i denoting the value of a at the first peak of the ϕ oscillations.

Since gravitational chargegenesis is only effective when ω deviates from -1 or $1/3$, the specific form of V in the slow-roll regime is not important in this work, as it only affects inflationary predictions. While the evolution of q_C is insensitive to the slow-roll part of the potential, it does depend on the shape of the potential close to its minimum, which can be modeled by a mass term. For concreteness, we adopt the following T -model potential [32, 33]¹

$$V(\phi) = 6\lambda \tanh^2\left(\phi/\sqrt{6}\right), \quad (7)$$

¹ The general form of T -model potentials is $V \propto \tanh^p(\phi/\sqrt{6})$, which approximates a broad class of models. For instance, the Starobinsky model approximately corresponds to $p = 2$.

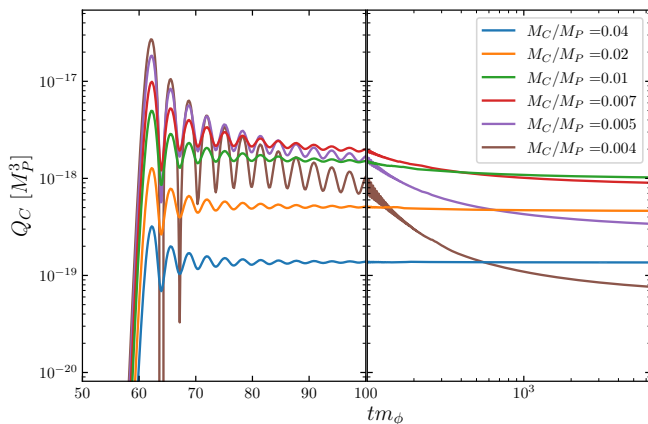


FIG. 1. Numerical solutions of Eq. (5) for different values of M_C . At $tm_\phi = 100$, we switch to a log scale on the tm_ϕ axis.

which reduces to $V(\phi) \approx 1/2 m_\phi^2 \phi^2$ with $m_\phi = \sqrt{2\lambda}$ at small ϕ . The slow-roll parameter $\epsilon = 1/2 (V'/V)^2$ for this potential is simply $\epsilon = 4/3 \text{csch}^2(\sqrt{2/3}\phi)$. The constant λ is determined by $\lambda \approx 18\pi^2 A_S / (6N_e^2)$ [33] where $N_e = 55$ is the number of e-folds and $A_S \approx 2.1 \times 10^{-9}$ [34].

We numerically solve Eqs. (3) to (5) starting from a point deep in the slow-roll regime with $\epsilon \ll 1$. Specifically, we set the initial point at $\phi = 6.13$, corresponding to $N_e = 55$, continuously evolve the system of equations through the end of slow-roll ($\epsilon = 1$), followed by a large number of inflaton oscillations, and stop at a sufficiently large time t , when Q_C has become constant. In Fig. 1, we present the numerical solutions for $M_* = 8.22 \times 10^{-5}$, $\Gamma_\phi = 1.23 \times 10^{-7}$, $n = 1$, and several values of M_C . We set $t = 0$ at $N_e = 55$ and denote quantities at the end of slow-roll by a subscript “*”. For the shown examples, $t_* \approx 59.4 m_\phi^{-1}$, $\phi_* \approx 1.21$, and $H_* \approx 3.3 \times 10^{-6}$.

During the slow-roll phase, Q_C cannot be significantly produced because $\omega \approx -1$, which leads to $Q_C^{\text{eq}} \propto \mu_A^{\text{eff}} \approx 0$. From the end of slow-roll to $t \sim \mathcal{O}(100) m_\phi^{-1}$, Q_C is effectively produced, with an oscillatory behavior driven by the oscillations of ϕ around the minimum of its potential. The oscillation frequency is of $\mathcal{O}(m_\phi)$. During the oscillatory phase, ϕ can be effectively viewed as a fluid with $\omega \approx 0$ due to $\langle p_\phi \rangle / \rho_\phi \approx 0$, implying an effective matter-dominated phase. As t further increases, Q_C asymptotically approaches a constant value. The oscillations in Q_C are eventually suppressed for two reasons: (i) ρ_ϕ gradually decays to ρ_R , driving the Universe towards complete radiation domination, and (ii) the decreasing temperature reduces the rate Γ_C , which hinders Q_C from following the rapid oscillations in Q_C^{eq} . Note that for the shown examples, Γ_C is always well below m_ϕ .

We now comment on the conditions under which the calculation can be trusted. Some further details can be found in the supplemental material S1. The effect of the interaction (1) on the cosmological expansion can be neglected if its contribution to the Friedmann equation

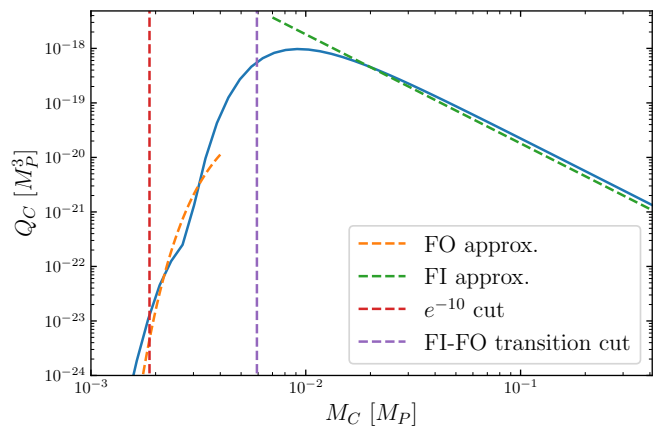


FIG. 2. Final value of Q_C as a function of M_C . The green and orange dashed lines represent the FI and FO approximate expressions in Eqs. (9) and (10), respectively. The purple and red dashed curves indicate the two cuts in Eq. (11).

is negligible, which leads to

$$M_*^2 \gg \frac{q_C m_\phi}{M_P^2}. \quad (8)$$

We verified that this condition is satisfied in our calculations. Furthermore, if the operator (1) arises from the low-energy expansion of a fundamental UV-complete theory, then additional constraints must be imposed to ensure that expansion parameters are under control. A necessary condition to suppress higher-dimensional operators arising from a weak-gravitational field expansion is $\mathcal{R}/M_*^2 \lesssim 1$. Additionally, $T\sqrt{\mathcal{R}}/M_*^2 \lesssim 1$ is required to suppress higher-dimensional derivative operators, see e.g. Refs. [10–13] and references therein for details. One can readily verify that our choice of parameters respects these constraints both during and after reheating.

III. FREEZE-IN/OUT AND PARAMETER SPACE

As is shown in Fig. 1, the production rate and final value of Q_C crucially depend on M_C . Here, we discuss two interesting regimes, in which the final value of Q_C can be understood analytically. For concreteness, the scope of the following discussion is restricted to charge-violating rates described by (6) with $n = 1$. Generalized expressions for $n \geq 1$ can be found in the supplemental material.

Freeze-in regime: For the examples shown in Fig. 1, the final value of Q_C scales like M_C^{-1} for $M_C \gtrsim 0.01 M_P$. In this regime, Q_C quickly approaches a constant due to reason (ii) discussed previously and we are in the freeze-in (FI) regime. Here, the final value of Q_C is determined by the charge produced during the first few inflaton oscillations. We find the following analytical expression (see

the supplemental material) for Q_C in this regime,

$$Q_C \approx \frac{m_\phi^{13/4} \phi_i^{13/4} \Gamma_\phi^{5/4}}{M_D^{3/4} M_*^2 M_C^2} \quad (\text{FI}), \quad (9)$$

where $M_D^{3/4} \approx 537 M_P^{3/4}$ and ϕ_i denotes the first peak value of $|\phi|$ during the oscillation phase. For $\Gamma_\phi \ll H$, we obtain $\phi_i \approx 0.3 M_P$, which is approximately a constant since the slow roll followed by the first oscillation is not significantly affected by Γ_ϕ .

Freeze-out regime: As M_C^{-1} is increased further, the asymmetry yield during the oscillatory phase will saturate an upper bound expected from the fluid approximation, which is roughly the average $\langle Q_C^{\text{eq}} \rangle$. On the other hand, large M_C^{-1} causes Q_C to be more tightly coupled to $\langle Q_C^{\text{eq}} \rangle$. When $\langle Q_C^{\text{eq}} \rangle$ is suppressed due to radiation domination ($\omega \approx 1/3$), the tight coupling will reduce the final value of Q_C . In this regime, we are able to derive

$$Q_C \approx \frac{\Gamma_\phi^2 m_\phi^2 \phi_i^2}{M_F M_*^2} \exp \left[-\frac{M_E^{3/2} \Gamma_\phi^{1/2}}{M_C^2} \right] \quad (\text{FO}), \quad (10)$$

where $M_E \approx 0.21 M_P$ and $M_F \approx 86 M_P$.

Analytically, one can estimate the value of M_C at the transition between freeze-in and freeze-out and also a lower bound of M_C below which Q_C is exponentially suppressed—see the supplemental material. Here we provide two useful cuts:

$$M_C \approx M_E^{3/4} \Gamma_\phi^{1/4} \times \begin{cases} 1.0 & \text{for FI-FO cut} \\ 0.3 & \text{for } e^{-10} \text{ cut} \end{cases}. \quad (11)$$

The FI-FO cut indicates the transition while the e^{-10} cut implies that the exponential in (10) leads to a suppression factor of e^{-10} .

In Fig. 2, we show the final value of Q_C as a function of M_C . One can see that the above analytical estimates agree well with the numerical result. We further perform a full numerical scan of the parameter space to identify the range of values of Γ_ϕ and M_C that can lead to successful gravitational chargegenesis. Fig. 3 shows the obtained result in terms of q_C/s where s is the entropy density. The top axis of Fig. 3 indicates the reheating temperature T_{rh} , which is defined as the temperature of the universe at the moment when $\rho_\phi = \rho_R$. This value is extracted directly from our numerical solutions while analytically one expects $T_{\text{rh}} \propto \Gamma_\phi^{1/2}$. Indeed, in our numerical solutions, we find $T_{\text{rh}} \approx 0.35 M_P^{1/2} \Gamma_\phi^{1/2}$ within the range of Γ_ϕ presented in Fig. 3.

Fig. 3 shows that the yield of charge asymmetry increases with increasing reheating temperature. However, if Γ_ϕ is too large, ϕ would decay even before the slow-roll ends, alternating the slow-roll paradigm. The Planck 2018 result constrains the Hubble parameter during inflation to be $H < 2.5 \times 10^{-5}$ at 95% CL [34], implying an upper bound on the reheating temperature, $T_{\text{rh}} < 6.6 \times 10^{15}$

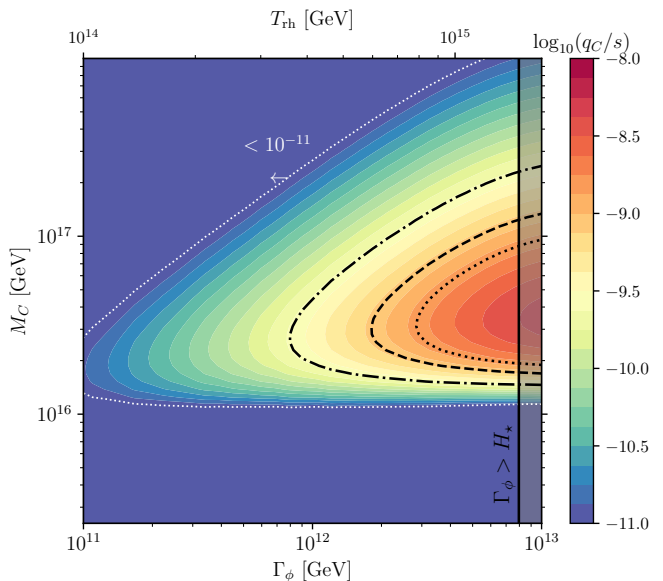


FIG. 3. Viable parameter space of gravitational chargegenesis. The black dashed contour ($q_C/s = 8.2 \times 10^{-10}$) can generate the observed baryon asymmetry assuming $|x_C| = 3/10$, while the dotted and dash-dotted contours assume $|x_C| = 1/6$ and 1. Larger Γ_ϕ generally leads to a higher yield of charge asymmetry, but overlarge Γ_ϕ would spoil the slow-roll predictions. Hence we cut off the scan when $\Gamma_\phi > H_*$, represented by the black solid line and the gray shaded region to the right.

GeV. If one naively extrapolates $T_{\text{rh}} \approx 0.35 M_P^{1/2} \Gamma_\phi^{1/2}$ to this scale, it can be interpreted as $\Gamma_\phi < 1.5 \times 10^{14}$ GeV. However, such a large Γ_ϕ would already exceed H_* and significantly modify the slow-roll evolution. Therefore, we conservatively set $\Gamma_\phi < H_* \approx 8 \times 10^{12}$ GeV as the upper bound of Γ_ϕ in Fig. 3.

In wash-in leptogenesis, the baryon asymmetry of the universe, $Y_B \equiv (n_B - n_{\bar{B}})/s$, is related to q_C by

$$Y_B = \frac{28}{79} x_C \frac{q_C}{s}, \quad (12)$$

where x_C is the coefficient relating the q_C asymmetry to the $B - L$ asymmetry. For electron asymmetry (q_e) produced before the electron Yukawa interaction reaches equilibrium around $T \sim 10^5$ GeV [35], we have $x_C = -3/10$ [4]. Hence to generate the observed value $Y_B \approx 8.7 \times 10^{-11}$ (see e.g. [36]), we need $|q_C|/s \approx 8.2 \times 10^{-10}$. This corresponds to the black dashed line in Fig. 3. For other charge asymmetries, we refer to Tab. II of Ref. [4], where $|x_C|$ typically varies from 1/6 to 1. The other two black contours demonstrate such variations.

We verified that by setting $n > 1$ in (6), a charge asymmetry sufficient to explain the BAU can be produced with lower values of M_C than in the $n = 1$ scenario. However, the allowed range for M_C becomes narrower compared to those restricted by the black curves in Fig. 3. Setting $n > 1$ also opens up the possibility of producing a sufficient charge asymmetry at lower reheating temperatures.

Finally, we also verified that for T -model potentials that can be approximated as $\sim \phi^p$, $p = 6, 8, 10, \dots$ during reheating, one can potentially reproduce the BAU in gravitational chargegenesis scenarios with significantly lower reheating temperatures than those indicated in Fig. 3. However, a consistent study of reheating potentials beyond the quadratic requires accounting for fragmentation of the inflaton condensate (see e.g. [37, 38]) and is left for future work.

IV. SUMMARY AND CONCLUSIONS

In this *letter*, we proposed a framework for chargegenesis, which, via wash-in leptogenesis, can explain the baryon asymmetry of the Universe. The two main ingredients are a gravitational interaction that dynamically generates effective chemical potentials and a charge-violating interaction that drives the plasma to a state with nonzero charge asymmetry q_C . In particular, we extend the scope of previous gravitational baryogenesis ideas by pointing out that the charge associated with the gravitational interaction and the charge that is being violated do not have to be the same. In the present framework, the generated charge does not even have to violate $B-L$ provided at least one right-handed neutrino is still active at a time when q_C is non vanishing.

As an application of the framework, we considered a concrete realization of gravitational chargegenesis after a period of slow-roll inflation where the inflaton oscillates around the minimum of its potential. We focused on the

simplest and most generic setup where the inflaton oscillates in a quadratic potential and provided a detailed time-resolved description of how q_C evolves throughout reheating and beyond. We showed that a sufficient charge to explain the baryon-asymmetry of the Universe can be generated while staying consistent with experimental constraints. As this mechanism, at least its most minimal realizations as considered here, generally requires a high inflation scale it also implies a large primordial tensor-to-scalar ratio in the cosmic microwave background power spectrum that could be detected by upcoming experiments. This renders gravitational chargegenesis an exciting possibility to pursue theoretically and experimentally.

Acknowledgements

M. A. M. thanks Hooman Davoudiasl for a pleasant conversation about gravitational baryogenesis, and Yong Xu for discussions about reheating. The work of K. S. is supported by Deutsche Forschungsgemeinschaft (DFG) through the Research Training Group (Graduiertenkolleg) 2149: Strong and Weak Interactions – from Hadrons to Dark Matter. M. A. M. acknowledges support from the DFG Collaborative Research Centre “Neutrinos and Dark Matter in Astro- and Particle Physics” (SFB 1258). The work of X. J. X is supported in part by the National Natural Science Foundation of China under grant No. 12141501 and also by the CAS Project for Young Scientists in Basic Research (YSBR-099).

-
- [1] **Planck** Collaboration, N. Aghanim *et al.*, “Planck 2018 results. VI. Cosmological parameters,” *Astron. Astrophys.* **641** (2020) A6, [arXiv:1807.06209 \[astro-ph.CO\]](#). [Erratum: *Astron. Astrophys.* 652, C4 (2021)].
 - [2] M. Fukugita and T. Yanagida, “Baryogenesis Without Grand Unification,” *Phys. Lett. B* **174** (1986) 45–47.
 - [3] D. Bodeker and W. Buchmuller, “Baryogenesis from the weak scale to the grand unification scale,” *Rev. Mod. Phys.* **93** no. 3, (2021) 035004, [arXiv:2009.07294 \[hep-ph\]](#).
 - [4] V. Domcke, K. Kamada, K. Mukaida, K. Schmitz, and M. Yamada, “Wash-In Leptogenesis,” *Phys. Rev. Lett.* **126** no. 20, (2021) 201802, [arXiv:2011.09347 \[hep-ph\]](#).
 - [5] V. Domcke, K. Kamada, K. Mukaida, K. Schmitz, and M. Yamada, “Wash-in leptogenesis after axion inflation,” *JHEP* **01** (2023) 053, [arXiv:2210.06412 \[hep-ph\]](#).
 - [6] K. Mukaida, H. Watanabe, and M. Yamada, “Thermal Wash-in Leptogenesis via Heavy Higgs Decay,” [arXiv:2405.14332 \[hep-ph\]](#).
 - [7] K. Schmitz and X.-J. Xu, “Wash-in leptogenesis after the evaporation of primordial black holes,” *Phys. Lett. B* **849** (2024) 138473, [arXiv:2311.01089 \[hep-ph\]](#).
 - [8] H. Davoudiasl, R. Kitano, G. D. Kribs, H. Murayama, and P. J. Steinhardt, “Gravitational baryogenesis,” *Phys. Rev. Lett.* **93** (2004) 201301, [arXiv:hep-ph/0403019](#).
 - [9] V. Domcke, Y. Ema, K. Mukaida, and M. Yamada, “Spontaneous Baryogenesis from Axions with Generic Couplings,” *JHEP* **08** (2020) 096, [arXiv:2006.03148 \[hep-ph\]](#).
 - [10] J. I. McDonald and G. M. Shore, “Gravitational leptogenesis, C, CP and strong equivalence,” *JHEP* **02** (2015) 076, [arXiv:1411.3669 \[hep-th\]](#).
 - [11] J. I. McDonald and G. M. Shore, “Leptogenesis from loop effects in curved spacetime,” *JHEP* **04** (2016) 030, [arXiv:1512.02238 \[hep-ph\]](#).
 - [12] J. I. McDonald and G. M. Shore, “Leptogenesis and gravity: baryon asymmetry without decays,” *Phys. Lett. B* **766** (2017) 162–169, [arXiv:1604.08213 \[hep-ph\]](#).
 - [13] J. I. McDonald and G. M. Shore, “Dynamical Evolution of Gravitational Leptogenesis,” *JHEP* **10** (2020) 025, [arXiv:2006.09425 \[hep-ph\]](#).
 - [14] R. Samanta and S. Datta, “Gravitational wave complementarity and impact of NANOGrav data on gravitational leptogenesis,” *JHEP* **05** (2021) 211, [arXiv:2009.13452 \[hep-ph\]](#).

- [15] R. Samanta and S. Datta, “Flavour effects in gravitational leptogenesis,” *JHEP* **12** (2020) 067, [arXiv:2007.11725 \[hep-ph\]](#).
- [16] R. Samanta and S. Datta, “Probing leptogenesis and pre-BBN universe with gravitational waves spectral shapes,” *JHEP* **11** (2021) 017, [arXiv:2108.08359 \[hep-ph\]](#).
- [17] P. Minkowski, “ $\mu \rightarrow e\gamma$ at a Rate of One Out of 10^9 Muon Decays?,” *Phys. Lett. B* **67** (1977) 421–428.
- [18] T. Yanagida, “Horizontal gauge symmetry and masses of neutrinos,” *Conf. Proc. C* **7902131** (1979) 95–99.
- [19] M. Gell-Mann, P. Ramond, and R. Slansky, “Complex Spinors and Unified Theories,” *Conf. Proc. C* **790927** (1979) 315–321, [arXiv:1306.4669 \[hep-th\]](#).
- [20] R. N. Mohapatra and G. Senjanovic, “Neutrino Mass and Spontaneous Parity Nonconservation,” *Phys. Rev. Lett.* **44** (1980) 912.
- [21] H. Li, M.-z. Li, and X.-m. Zhang, “Gravitational leptogenesis and neutrino mass limit,” *Phys. Rev. D* **70** (2004) 047302, [arXiv:hep-ph/0403281](#).
- [22] B. Feng, H. Li, M.-z. Li, and X.-m. Zhang, “Gravitational leptogenesis and its signatures in CMB,” *Phys. Lett. B* **620** (2005) 27–32, [arXiv:hep-ph/0406269](#).
- [23] G. Lambiase and G. Scarpetta, “Baryogenesis in $f(R)$: Theories of Gravity,” *Phys. Rev. D* **74** (2006) 087504, [arXiv:astro-ph/0610367](#).
- [24] G. Lambiase, S. Mohanty, and A. R. Prasanna, “Neutrino coupling to cosmological background: A review on gravitational Baryo/Leptogenesis,” *Int. J. Mod. Phys. D* **22** (2013) 1330030, [arXiv:1310.8459 \[hep-ph\]](#).
- [25] V. K. Oikonomou and E. N. Saridakis, “ $f(T)$ gravitational baryogenesis,” *Phys. Rev. D* **94** no. 12, (2016) 124005, [arXiv:1607.08561 \[gr-qc\]](#).
- [26] S. D. Odintsov and V. K. Oikonomou, “Gauss–Bonnet gravitational baryogenesis,” *Phys. Lett. B* **760** (2016) 259–262, [arXiv:1607.00545 \[gr-qc\]](#).
- [27] M. P. L. P. Ramos and J. Páramos, “Baryogenesis in Nonminimally Coupled $f(R)$ Theories,” *Phys. Rev. D* **96** no. 10, (2017) 104024, [arXiv:1709.04442 \[gr-qc\]](#).
- [28] S. Bhattacharjee and P. K. Sahoo, “Baryogenesis in $f(Q, T)$ gravity,” *Eur. Phys. J. C* **80** no. 3, (2020) 289, [arXiv:2002.11483 \[physics.gen-ph\]](#).
- [29] A. De Simone, T. Kobayashi, and S. Liberati, “Geometric Baryogenesis from Shift Symmetry,” *Phys. Rev. Lett.* **118** no. 13, (2017) 131101, [arXiv:1612.04824 \[hep-ph\]](#).
- [30] Q. Liang, J. Sakstein, and M. Trodden, “Baryogenesis via gravitational spontaneous symmetry breaking,” *Phys. Rev. D* **100** no. 6, (2019) 063518, [arXiv:1904.10510 \[hep-ph\]](#).
- [31] M. S. Turner, “Coherent Scalar Field Oscillations in an Expanding Universe,” *Phys. Rev. D* **28** (1983) 1243.
- [32] R. Kallosh and A. Linde, “Universality Class in Conformal Inflation,” *JCAP* **07** (2013) 002, [arXiv:1306.5220 \[hep-th\]](#).
- [33] B. Barman, S. Cléry, R. T. Co, Y. Mambrini, and K. A. Olive, “Gravity as a portal to reheating, leptogenesis and dark matter,” *JHEP* **12** (2022) 072, [arXiv:2210.05716 \[hep-ph\]](#).
- [34] **Planck** Collaboration, Y. Akrami *et al.*, “Planck 2018 results. X. Constraints on inflation,” *Astron. Astrophys.* **641** (2020) A10, [arXiv:1807.06211 \[astro-ph.CO\]](#).
- [35] D. Bödeker and D. Schröder, “Equilibration of right-handed electrons,” *JCAP* **05** (2019) 010, [arXiv:1902.07220 \[hep-ph\]](#).
- [36] S. Davidson, E. Nardi, and Y. Nir, “Leptogenesis,” *Phys. Rept.* **466** (2008) 105–177, [arXiv:0802.2962 \[hep-ph\]](#).
- [37] K. D. Lozanov and M. A. Amin, “Equation of State and Duration to Radiation Domination after Inflation,” *Phys. Rev. Lett.* **119** no. 6, (2017) 061301, [arXiv:1608.01213 \[astro-ph.CO\]](#).
- [38] K. D. Lozanov and M. A. Amin, “Self-resonance after inflation: oscillons, transients and radiation domination,” *Phys. Rev. D* **97** no. 2, (2018) 023533, [arXiv:1710.06851 \[astro-ph.CO\]](#).
- [39] K. D. Lozanov, “Lectures on Reheating after Inflation,” [arXiv:1907.04402 \[astro-ph.CO\]](#).

Supplemental Material

S1. EXPANSION OF THE UNIVERSE

In this supplementary material, we provide some details about the consistency of our framework. The theory under consideration has the following schematic action,

$$S = \int d^4x \sqrt{-g} \left[\frac{\mathcal{R}}{2} M_P^2 \left(1 - \frac{2 \partial_\mu J_C^\mu}{M_*^2 M_P^2} \right) + \mathcal{L}_M \right] + \dots \quad (\text{S1})$$

where we have discarded a total derivative and additional gravitational operators that may appear in a more complete model description. Here \mathcal{L}_M denotes the non-gravitational interactions in the Lagrangian.

The standard Einstein equation is recovered by discarding the current operator and varying (S1) with respect to the metric. The Friedmann equation, which determines the expansion of the universe, is simply the (0,0) component of Einstein's equation. In the presence of the current operator, the Friedmann equation is modified. A simple calculation reveals that the modification is negligible if

$$\frac{\dot{q}_C}{M_*^2 M_P^2} \ll 1. \quad (\text{S2})$$

The charge q_C is negligible during inflation, and starts to rapidly oscillate with a period set by the inflaton mass m_ϕ during the early stages of reheating, as shown in Fig. 1. Hence, requiring the current-operator under study to have negligible impact on the expansion of the universe leads to the constraint in (8).

S2. ANALYTICAL RESULTS

In this supplementary material, we present the explicit derivation of the analytical results used in this work.

A. Analytical expressions for ϕ , ρ_ϕ , and ρ_R

During a matter-dominated era, the Hubble parameter is approximately given by $H \approx \frac{2}{3t}$. Since $\frac{2}{3t}$ is divergent at $t \rightarrow 0$, we regulate it by shifting the beginning of matter domination away from $t = 0$ to $t = t_i$:

$$H \approx \frac{1}{H_i^{-1} + \frac{3(t-t_i)}{2}}, \quad (\text{S3})$$

such that the transition from an inflationary epoch to matter domination happens around $t = t_i$ and H_i denotes the Hubble parameter at this transition.

The universe is in a matter-dominated state when ϕ oscillates at the bottom of its potential. We define t_i as the moment when ϕ reaches the first peak of the oscillations. We denote the corresponding values of ϕ , H , and a at this moment by ϕ_i , H_i , and a_i , respectively. For convenience, we also define the following two dimensionless quantities:

$$h_m \equiv \frac{H_i}{m_\phi}, \quad \theta_t \equiv m_\phi(t - t_i). \quad (\text{S4})$$

By definition, we have $\dot{\phi}(t_i) = 0$, which implies $\rho_\phi(t_i) = m_\phi^2 \phi_i^2 / 2$ and $H_i \approx M_P^{-1} \sqrt{\rho_\phi / 3} \approx M_P^{-1} m_\phi |\phi_i| / \sqrt{6}$, assuming $\rho_R \ll \rho_\phi$ at $t = t_i$. Hence, h_m and ϕ_i are related by

$$h_m = \frac{|\phi_i|}{\sqrt{6} M_P}, \quad \text{or} \quad |\phi_i| = \sqrt{6} h_m M_P. \quad (\text{S5})$$

From Eq. (S3), it is straightforward to compute the scale factor by solving $\dot{a}/a = H$. Writing the approximate expressions of H and a in terms of h_m and θ_t , we obtain

$$a \approx a_i \left(1 + \frac{3}{2} h_m \theta_t \right)^{\frac{2}{3}}, \quad (\text{S6})$$

$$H \approx \frac{2 m_\phi h_m}{3 h_m \theta_t + 2}. \quad (\text{S7})$$

Substituting Eq. (S7) into Eq. (3) and using the quadratic expansion of V , one can solve Eq. (3) analytically in the limit of $\Gamma_\phi \rightarrow 0$ and obtain

$$\phi \approx \frac{2 \phi_i}{3 h_m \theta_t + 2} \cos \theta_t, \quad (\text{S8})$$

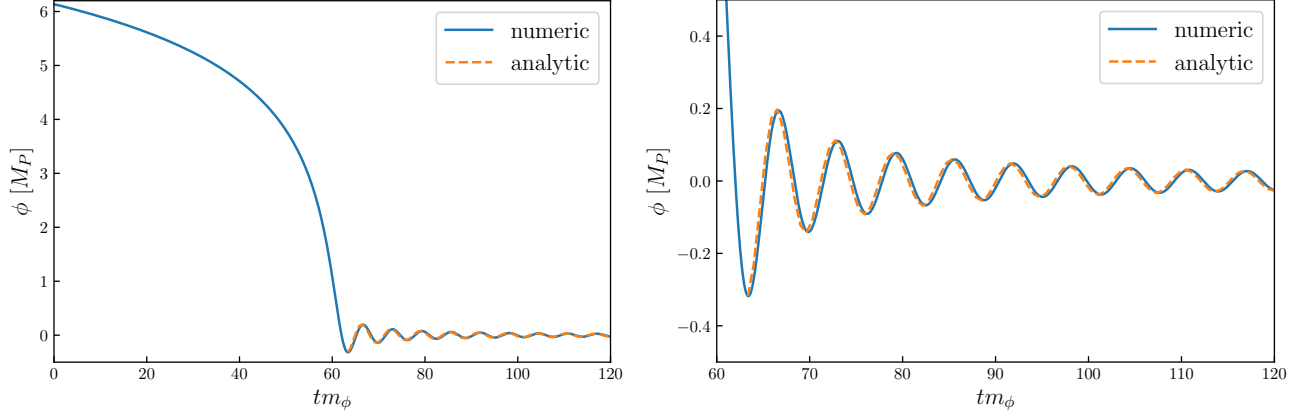


FIG. S1. The analytic solution in Eq. (S8) compared with the full numeric solution obtained by solving Eq. (3) with the T-model potential in Eq. (7). The right panel is simply a zoom-in view of the left.

which agrees well with the numerical solution. Figure S1 shows the accuracy of the above approximate solution for ϕ as a function of time for $t \geq t_i$. The numerical solution (blue curve) in this plot is obtained by solving Eq. (3) with the T-model potential in Eq. (7) and $\Gamma_\phi = 0$.

From Eq. (S8), one can derive an analytic approximation for ρ_ϕ

$$\rho_\phi \approx \frac{2m_\phi^2 \phi_i^2}{(3h_m \theta_t + 2)^2} [1 + h_t \sin 2\theta_t + (h_t \cos \theta_t)^2], \quad (\text{S9})$$

where $h_t \equiv \frac{3h_m}{3h_m \theta_t + 2}$. In Eq. (S9), the three terms are proportional to h_t^0 , h_t^1 and h_t^2 with $h_t \ll 1$. Hence, ρ_ϕ does not exhibit large oscillations as the second and third oscillatory terms are quickly suppressed at large t . However, this is not the case for \dot{R} computed from ρ_ϕ and its time derivatives ($\dot{\rho}_\phi$, $\ddot{\rho}_\phi$), as we will show later. Therefore, the oscillatory terms in Eq. (S9) remain important for subsequent calculations.

It is worth mentioning here that if we treat ϕ in the oscillation phase as a fluid with $\omega_\phi = 0$, we would obtain an analytical expression for ρ_ϕ corresponding to the non-oscillatory term in Eq. (S9). More specifically, in the fluid approximation, Eq. (3) can be recast as

$$\dot{\rho}_\phi + (3H + \Gamma_\phi)(1 + \omega_\phi)\rho_\phi = 0. \quad (\text{S10})$$

By setting $\Gamma_\phi = \omega_\phi = 0$ and using Eq. (S7), we obtain

$$\rho_\phi \approx 3 \left(\frac{2M_P m_\phi h_m}{3h_m \theta_t + 2} \right)^2, \quad (\text{S11})$$

which is exactly the first term in Eq. (S9).

Next, we consider Eq. (4) for ρ_R . If $\dot{\rho}_R \ll 4H\rho_R$, we can ignore the $\dot{\rho}_R$ term in Eq. (4) and obtain

$$\rho_R \approx \frac{\Gamma_\phi(1 + \omega_\phi)\rho_\phi}{4H} \approx \frac{3m_\phi \Gamma_\phi h_m M_P^2}{2(3h_m \theta_t + 2)}, \quad (\text{assuming } \dot{\rho}_R \ll 4H\rho_R), \quad (\text{S12})$$

where we have used Eq. (S11) and $\omega_\phi = 0$. However, we find that $\dot{\rho}_R \ll 4H\rho_R$ is actually not a very good approximation as Eq. (S12) would imply

$$\dot{\rho}_R \approx -\frac{3h_m m_\phi}{3h_m \theta_t + 2} \rho_R, \quad (\text{assuming } \dot{\rho}_R \ll 4H\rho_R). \quad (\text{S13})$$

For $\theta_t = 0$ and $h_m \theta_t \gg 1$, Eq. (S13) gives $|\dot{\rho}_R| \approx 3H_i \rho_R$ and $|\dot{\rho}_R| \approx \rho_R/t \approx 3H\rho_R/2$, respectively. Both are smaller than $4H\rho_R$ but not much smaller than $4H\rho_R$. To improve the approximation, we substitute Eq. (S13) into Eq. (4) to account for the contribution from the $\dot{\rho}_R$ term. The resulting equation reads

$$\left(-\frac{3h_m m_\phi}{3h_m \theta_t + 2} + 4H \right) \rho_R = \Gamma_\phi(1 + \omega_\phi)\rho_\phi, \quad (\text{S14})$$

which upon substitution of $\omega_\phi = 0$ yields

$$\rho_R = \frac{12\Gamma_\phi M_P^2 m_\phi h_m}{5(3h_m \theta_t + 2)}. \quad (\text{S15})$$

In Figure S2, we display a comparison of the analytical results in Eqs. (S11) and (S15) with full numerical results, for $\Gamma_\phi \approx 4.11 \times 10^{-9} M_P$. As can be seen in the figure, Eqs. (S11) and (S15) describe the evolution of ρ_ϕ and ρ_R accurately before the universe transitions from ρ_ϕ domination to ρ_R domination.

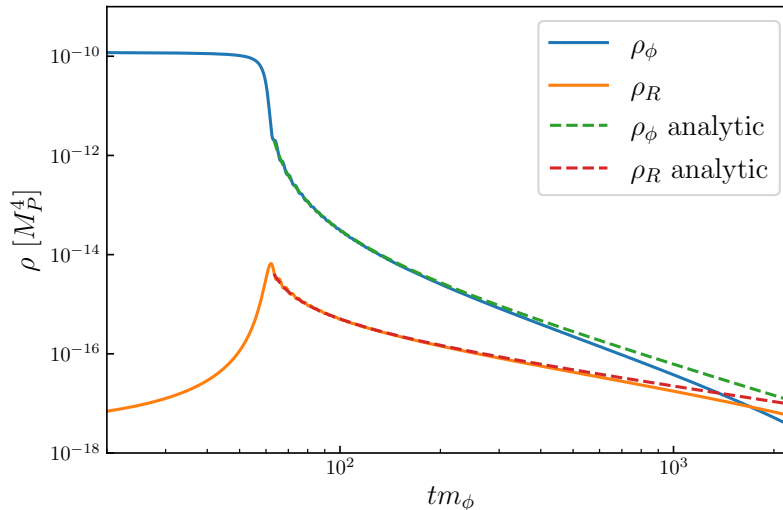


FIG. S2. Evolution of ρ_ϕ and ρ_R . Solid lines are computed in the full numerical approach, while dashed lines are obtained using Eqs. (S11) and (S15).

B. Analytical expressions for \mathcal{R} and $\dot{\mathcal{R}}$

In the $(+, - - -)$ metric convention, the Ricci scalar \mathcal{R} in the FRW Universe is given by

$$\mathcal{R} = -6 \left[\frac{\ddot{a}}{a} + \left(\frac{\dot{a}}{a} \right)^2 \right] = -6 \left[\dot{H} + 2H^2 \right]. \quad (\text{S16})$$

The time-derivative of the Ricci scalar is readily obtained by applying the second Friedmann equation,

$$\dot{\mathcal{R}} = \frac{3\rho\dot{\omega}}{M_P^2} + \frac{\sqrt{3}(1+\omega)(1-3\omega)}{M_P^3} \rho^{3/2}. \quad (\text{S17})$$

By substituting Eq. (S7) into Eq. (S16) and evaluating the time derivative, we obtain the following analytical results

$$\mathcal{R} \approx -\frac{12h_m^2 m_\phi^2}{(3h_m \theta_t + 2)^2}, \quad (\text{S18})$$

$$\dot{\mathcal{R}} \approx \frac{72h_m^3 m_\phi^3}{(3h_m \theta_t + 2)^3}, \quad (\text{S19})$$

which are valid during reheating. Eqs. (S18) and (S19) should be considered as leading approximations that do not account for oscillations. To arrive at a more accurate description, we now incorporate the oscillatory terms in ρ_ϕ into \mathcal{R} and $\dot{\mathcal{R}}$, as shown in the following.

Given the explicit expression of ρ and its derivatives $(\dot{\rho}, \ddot{\rho})$, Eq. (S16) can be used to directly compute \mathcal{R} . This is most easily seen by recalling that $H = M_P^{-1} \sqrt{\rho/3}$ and $\dot{H} = M_P^{-1} d(\sqrt{\rho/3})/dt$, i.e. all relevant quantities can be written in terms of ρ and its time derivatives. Hence, starting from

$$\mathcal{R} = -\frac{4\rho + \dot{\rho}/H}{M_P^2}, \quad (\text{S20})$$

and taking $\rho \approx \rho_\phi$, substituting Eqs. (S9) and (S7) into Eq. (S20), neglecting a few subdominant terms such as the h_i^2 term in Eq. (S9), we eventually obtain

$$\mathcal{R} \approx -\frac{2m_\phi^2 \phi_i^2}{M_P^2 (3h_m \theta_t + 2)^2} [1 + 3 \cos(2\theta_t)]. \quad (\text{S21})$$

The time derivative of Eq. (S21) gives

$$\dot{\mathcal{R}} \approx \frac{12m_\phi^3 \phi_i^2}{M_P^2 (3\theta_t h_m + 2)^2} \left[\sin 2\theta_t + \frac{h_m}{3\theta_t h_m + 2} (1 + 3 \cos 2\theta_t) \right]. \quad (\text{S22})$$

If we average out the $\sin 2\theta_t$ and $\cos 2\theta_t$ terms in Eq. (S22), $\dot{\mathcal{R}}$ reduces exactly to Eq. (S19), as expected.

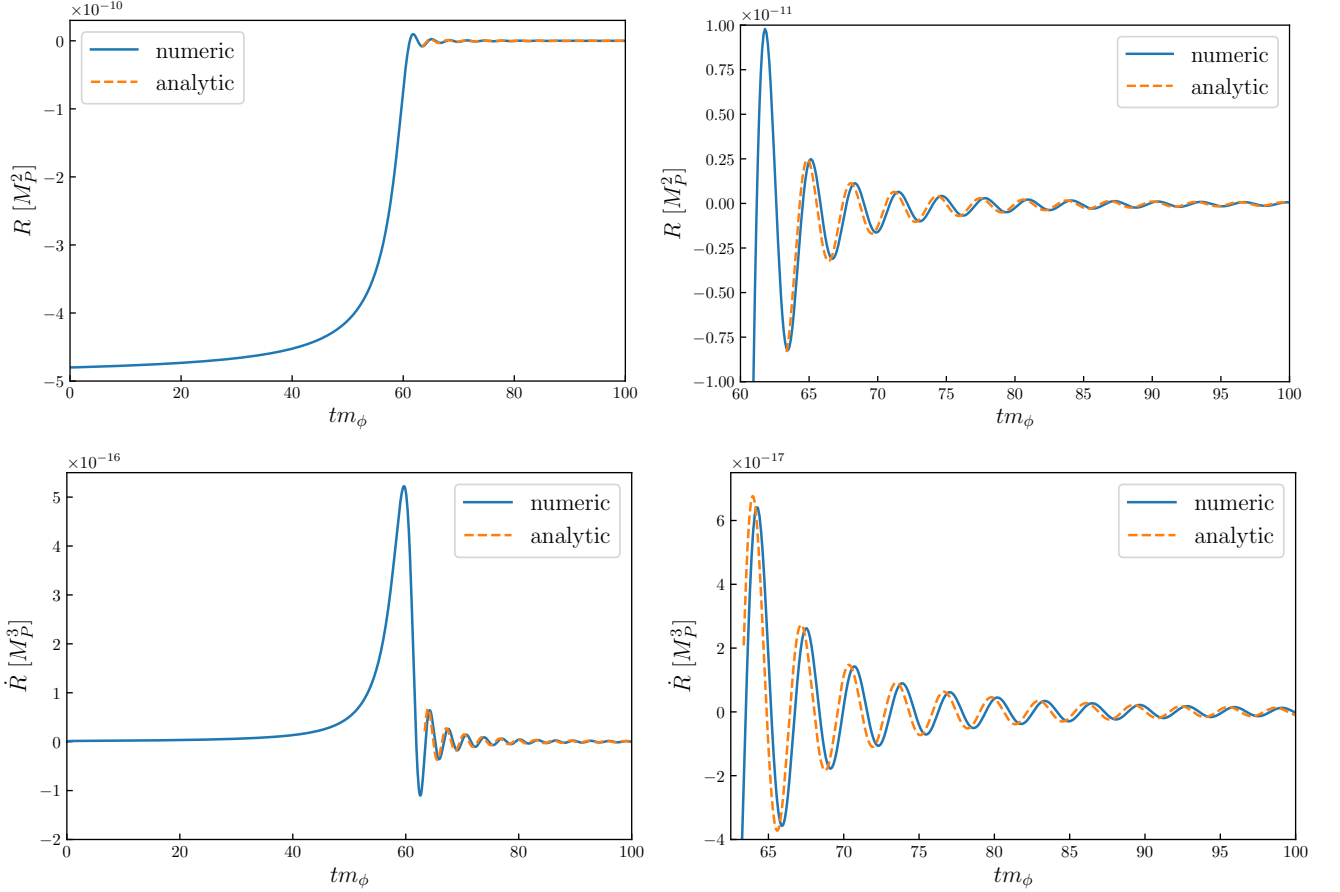


FIG. S3. The analytic expressions in Eqs. (S21) and (S22) for \mathcal{R} (upper panels) and $\dot{\mathcal{R}}$ (lower panels), compared with the full numerical results obtained by solving Eq. (3) with the T-model potential in Eq. (7). The right panels are simply zoom-in views of the left.

Finally, we note that Eq. (S21) is similar to Eq. (4.22) in [39], but our result contains an extra factor “+2” in the denominator, which yields a more accurate approximation at small θ_i . In Fig. S3, we plot Eqs. (S21) and (S22), and compare them with full numerical results obtained by solving Eq. (3) with $\Gamma_\phi = 0$. As is shown in the figure, the analytical expressions agree well with the numerical results.

C. The freeze-in and freeze-out values of Q_C

Next, we consider analytical approximations of Q_C for the freeze in and the freeze out regimes. By defining $Q_C \equiv q_C a^3/a_i^3$ and $Q_C^{\text{eq}} \equiv q_C^{\text{eq}} a^3/a_i^3$, one can rewrite Eq. (5) as

$$\frac{dQ_C}{dt} = \Gamma_C Q_C^{\text{eq}} - \Gamma_C Q_C. \quad (\text{S23})$$

According to Appendix B in [7], the solution for this equation can be formally written as

$$Q_C(t) = G(t) \int_0^t \frac{\Gamma_C(t') Q_C^{\text{eq}}(t')}{G(t')} dt', \quad G(t) \equiv \exp \left[- \int_0^t \Gamma_C(t') dt' \right]. \quad (\text{S24})$$

In the limit of $\Gamma_C \rightarrow 0$, i.e. the freeze-in regime, we have $G \rightarrow 1$ and thus

$$Q_C \approx \int \Gamma_C Q_C^{\text{eq}} dt \approx \int \dot{R} K dt, \quad K \equiv \frac{(a/a_i)^3 T^{2n+3}}{6M_*^2 M_C^{2n}}. \quad (\text{S25})$$

Here, the temperature T can be determined from ρ_R ,

$$T = \left(\frac{30}{\pi^2 g_*} \rho_R \right)^{1/4} = c_g \rho_R^{1/4} \quad \text{with} \quad c_g \equiv \left(\frac{30}{\pi^2 g_*} \right)^{1/4} \approx 0.41, \quad (\text{S26})$$

where the number of effective relativistic degrees of freedom g_* in the standard model is $g_* = 106.75$ at the temperature scales relevant to our work. By combining the analytical results (S6), (S15), and (S22), we get

$$\dot{R}K \approx \frac{m_\phi^3 \phi_i^2}{2M_*^2 M_C^{2n} M_P^2} \left(\frac{h_m}{3h_m \theta_t + 2} \right) \left(\frac{72 \Gamma_\phi M_P^2 m_\phi h_m}{\pi^2 g_* (3h_m \theta_t + 2)} \right)^{\frac{2n+3}{4}} \left[1 + 3 \cos 2\theta_t + \frac{3\theta_t h_m + 2}{h_m} \sin 2\theta_t \right]. \quad (\text{S27})$$

By neglecting oscillatory terms and integrating from $t = t_i$ (corresponding to $\theta_t = 0$) to $t = \infty$, we obtain

$$\int_{\cancel{\neq} t} \dot{R}K dt \approx \frac{2}{3(2n+3)} \frac{m_\phi^2 \phi_i^2}{M_*^2 M_C^{2n} M_P^2} \left(\frac{36 \Gamma_\phi M_P^2 m_\phi h_m}{\pi^2 g_*} \right)^{\frac{2n+3}{4}}, \quad (\text{S28})$$

where “ $\cancel{\neq}$ ” reminds us that we have neglected the $\sin 2\theta_t$ and $\cos 2\theta_t$ terms in Eq. (S27). To quantify the deviation of this simplified result from the full result, which accounts for oscillations in $\dot{R}K$, we define the following quantity

$$r_h \equiv \frac{\int_{\cancel{\neq} t} \dot{R}K dt}{\int \dot{R}K dt} = \frac{\int_0^\infty d\theta_t (3h_m \theta_t + 2)^{-(2n+7)/4}}{\int_0^\infty d\theta_t (3h_m \theta_t + 2)^{-(2n+7)/4} \left[1 + 3 \cos 2\theta_t + \frac{3\theta_t h_m + 2}{h_m} \sin 2\theta_t \right]}, \quad (\text{S29})$$

which is only a function of h_m . For $h_m \ll 1$, we find that r_h varies within a quite narrow range, typically between 0.34 and 0.35 for $n = 1$. Finally, by combing the expressions above, we obtain the freeze-in value of Q_C :

$$Q_C \approx \frac{1}{r_h} \frac{2}{3(2n+3)} \frac{m_\phi^2 \phi_i^2}{M_*^2 M_C^{2n} M_P^2} \left(\frac{36 \Gamma_\phi M_P^2 m_\phi h_m}{\pi^2 g_*} \right)^{\frac{2n+3}{4}} \quad (\text{for freeze-in}). \quad (\text{S30})$$

When Γ_C is too large, the approximations used to derive the freeze-in value are no longer valid but one can analytically estimate Q_C in the freeze-out regime. During freeze out, we assume that Q_C is tightly coupled to Q_C^{eq} until the universe enters the ρ_R dominated era, in which Q_C^{eq} quickly vanishes because ρ_ϕ decays exponentially in the subsequent evolution. Under this assumption, we are only concerned with the evolution of Q_C starting from the point when $\rho_R = \rho_\phi$.

By equating Eq. (S11) to (S15), we obtain an approximate value for θ_t at the time when ρ_R becomes equal to ρ_ϕ ,

$$\theta_t \approx \frac{5m_\phi h_m - 2\Gamma_\phi}{3\Gamma_\phi h_m} \quad (\text{for } \rho_R = \rho_\phi). \quad (\text{S31})$$

Using Eq. (S31) and assuming that the oscillating terms in Q_C^{eq} are negligible, we obtain

$$\langle Q_C^{\text{eq}} \rangle \approx \frac{\sqrt{3} c_g^2 \Gamma_\phi^2 m_\phi^2 \phi_i^2}{25 M_P M_*^2} \quad (\text{at } \rho_R = \rho_\phi), \quad (\text{S32})$$

where c_g has been defined in Eq. (S26). Once ρ_R increases across ρ_ϕ , Q_C^{eq} will drop exponentially as t becomes comparable to Γ_ϕ^{-1} . Meanwhile, Q_C decreases at a much lower rate determined by Γ_C . The subsequent part of the evolution is no longer sensitive to Q_C^{eq} , which can safely be set to zero. Eventually Q_C will reach a stable value when $\Gamma_C \ll H$. Under this assumption, we apply the formalism in Eq. (S24) to the period starting from $\rho_R = \rho_\phi$ and integrate t out to infinity. This results in

$$Q_C \approx \langle Q_C^{\text{eq}} \rangle \exp \left[-\frac{\sqrt{3}}{2n-1} \left(\frac{2\sqrt{3}}{5} \right)^{\frac{2n-1}{2}} \frac{c_g^{2n+1} M_P^{\frac{2n+1}{2}} \Gamma_\phi^{\frac{2n-1}{2}}}{M_C^{2n}} \right] \quad (\text{for freeze-out}). \quad (\text{S33})$$

If M_C is very small, then Q_C in Eq. (S33) would be exponentially suppressed. To estimate the magnitude of M_C for when the exponential suppression becomes highly efficient, we solve the following equation,

$$\frac{Q_C}{\langle Q_C^{\text{eq}} \rangle} = e^{-10}, \quad (\text{S34})$$

which gives

$$M_C = \left(\frac{\sqrt{3}}{10(2n-1)} \right)^{\frac{1}{2n}} \left(\frac{2\sqrt{3}}{5} \right)^{\frac{2n-1}{4n}} \sqrt{c_g^2 M_P \Gamma_\phi} \left(\frac{c_g^2 M_P}{\Gamma_\phi} \right)^{\frac{1}{4n}}. \quad (\text{S35})$$

We refer to this M_C value as the e^{-10} cut, or M_C^{cut} , below which Q_C is expected to be suppressed by at least a factor of $e^{-10} \sim 10^{-5}$ compared to Q_C^{eq} at $\rho_R = \rho_\phi$.

One can estimate the transition from the freeze-in to the freeze-out regime by introducing a transition value M_C^{trans} for which the argument of the exponential in (S33) equals -1 . This definition implies the following relation

$$M_C^{\text{trans}} = 10^{\frac{1}{2n}} M_C^{\text{cut}}, \quad (\text{S36})$$

which manifests the fact that the FO window becomes narrower for increasing n , as mentioned in the main text.

S3. SLOW-ROLL PARAMETERS

When adopting the T-model potential in Eq. (7), the slow-roll parameters can be obtained in compact analytical forms,

$$\epsilon \equiv \frac{M_P^2}{2} \left(\frac{V'}{V} \right)^2 = \frac{4}{3} \operatorname{csch}^2 \left(\sqrt{\frac{2}{3}} \frac{\phi}{M_P} \right), \quad (\text{S37})$$

$$\eta \equiv M_P^2 \left(\frac{V''}{V} \right) = \frac{4}{3} \left[2 - \cosh \left(\sqrt{\frac{2}{3}} \frac{\phi}{M_P} \right) \right] \operatorname{csch}^2 \left(\sqrt{\frac{2}{3}} \frac{\phi}{M_P} \right). \quad (\text{S38})$$

$$(\text{S39})$$

The number of e-folds is given by

$$N_e \equiv \frac{1}{\sqrt{2}M_P} \int_{\phi_e}^{\phi} \frac{d\phi'}{\sqrt{\epsilon(\phi')}} = \frac{3}{4} \cosh \left(\sqrt{\frac{2}{3}} \frac{\phi}{M_P} \right) - \frac{3}{4} \cosh \left(\sqrt{\frac{2}{3}} \frac{\phi_e}{M_P} \right), \quad (\text{S40})$$

where ϕ_e denotes ϕ at the end of inflation.